DOI: 10.1002/adma.200601455

Fine Tuning of the Face Orientation of ZnO Crystals to Optimize Their Photocatalytic Activity**

By *Eue Soon Jang*, *Jung-Hee Won*, *Seong-Ju Hwang*, and *Jin-Ho Choy**

Since environmental pollution has exceeded the limit of natural purification,[1] semiconductor-based photocatalytic reactions have attracted intense interest as an effective way of purifying air and water contaminants.[2] Among the various semiconductors, zinc oxide, with a direct wide bandgap ($\Delta E = 3.37$ eV), is of special importance for the photocatalytic generation of hydrogen peroxide,[3] which can be utilized for the degradation of organic pollutants and the sterilization of bacteria and viruses.[2,4] Due to the fact that a photocatalytic reaction occurs at the interface between catalyst surfaces and organic pollutants,[2] it is highly feasible that the photocatalytic activity of ZnO is strongly dependent on the growth direction of the crystal plane. Such speculation gives us the impetus to explore the relationship between surface orientation of ZnO crystals and their photocatalytic efficiency. However, due to an intrinsic anisotropy in the growth rate v of ZnO, with $v[0001] \gg v[01\bar{1}0] > v[000\bar{1}]$, hexagonal rods elongated along the *c*-axis have been predominantly synthesized.[5,6] Such an anisotropic tendency in crystal growth makes it difficult to directly probe the relationship between face orientation and photocatalytic activity. Here we report the novel face-tunable synthesis of nano- and microscale ZnO crystals with different ratios of polar to nonpolar faces. With these morphology-controlled crystals, we were able to clearly demonstrate a strong dependence of photocatalytic activity on a specific crystal plane.

In Figure 1, we show schematic models for face-tunable synthetic routes to ZnO crystals. The morphologies of the resulting ZnO crystals were investigated with field-emission scanning electron microscopy (FESEM), as shown in Figure 2, and the theoretical surface areas of four different samples, estimated from the FESEM results, are summarized in Table 1.

Table 1. Crystallite dimensions: estimated areas of total and Zn (0001) faces of nanoplates, nanorods, microrods, and DB microrods of zinc oxide.

	Average diameter [μm]	Average thickness [μm]	Calculated area of total surface [m^2g^{-1}]	Calculated area of Zn (0001) face [m^2g^{-1}]
Nanoplates	1.00	0.05	7.70	3.53
Nanorods	0.10	1.50	8.30	0.12
Microrods	1.80	6.20	0.50	0.03
DB microrods	3.50	6.00	0.25	–

First, hexagonal ZnO nanorods were prepared simply by hydrothermal treatment of dip-coated ZnO nanoparticles on a Si wafer with a uniform size of 4 nm (Fig. 1a).[6a] The corresponding FESEM image of Figure 2a reveals the formation of a dense array of ZnO nanorods with a uniform diameter of 100 nm and a length of 1.5 μm. Due to a one-dimensional nanostructure extended along the [0001] direction, the ZnO nanorods have a larger population of nonpolar $\{01\bar{1}0\}$ faces than polar {0001} ones. In order to suppress crystal growth along the [0001] axis, we tried to protect the Zn^{2+}-terminated (0001) plane, that is, Zn (0001), through complexation between Zn^{2+} ions and citrate ligands.[7] On the basis of this strategy, hexagonal nanoplates with a uniform diameter of 1.0 μm and a thickness of 50 nm were successfully obtained, as can be seen clearly from the FESEM image in Figure 2b. Such formation of nanoplates with a high proportion of polar {0001} planes is surely due to a strong suppression of crystal growth along the [0001] axis with a relative enhancement of crystal growth along the $[01\bar{1}0]$ direction, as illustrated in Figure 1b. Similarly, the tailored synthesis of diverse ZnO nanostructures was accomplished using controlled seeded growth of zinc oxide with citrate anions. The ZnO nanocolumns, consisting of the one-dimensional stacked nanoplates, were found to show enhanced photocatalytic activity towards the decomposition of 4-chlorophenol.[8] In contrast to nanocrystals, microcrystalline homologues could be prepared without nanocrystalline ZnO seeds (Fig. 1c). A hydrothermal reaction of zinc acetate under basic conditions resulted in prismatic ZnO microrods, as shown in Figure 2c. Due to an increase in particle size, the area of nonpolar $\{01\bar{1}0\}$ planes in this microrod

[*] Prof. J.-H. Choy, Prof. S. J. Hwang
Center for Intelligent Nano-Bio Materials (CINBM)
Division of Nano Sciences and Department of Chemistry
Ewha Womans University
Seoul 120-750 (Korea)
E-mail: jhchoy@ewha.ac.kr
Dr. E. S. Jang
Emerging Technology Research Department
Advanced Technology Laboratory, Korea Telecom (KT)
Seoul 137-792 (Korea)
J.-H. Won
Program in Nano-science and Technology
Seoul National University
Seoul 151-742 (Korea)

[**] This work was supported by the SRC/ERC program of MOST/KOSEF (grant: R11-2005-008-01001-0). Supporting Information is available online from Wiley InterScience or from the author.

ADVANCED MATERIALS

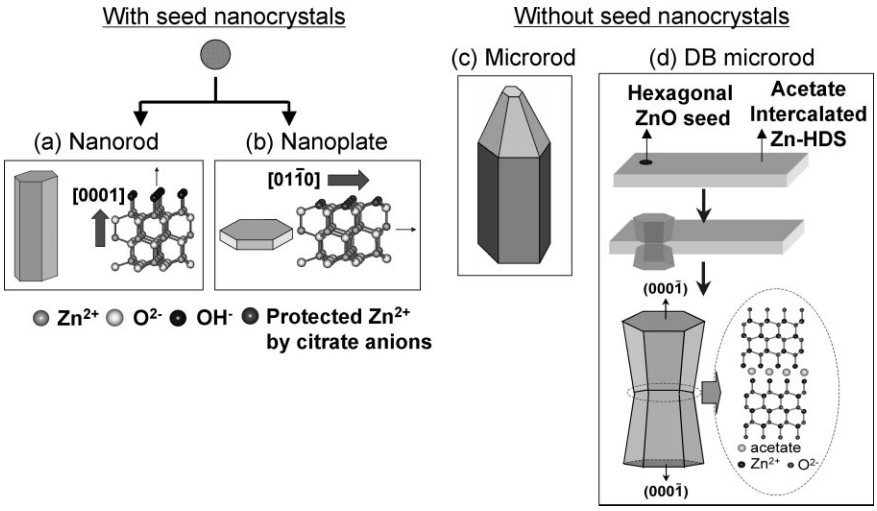

Figure 1. Schematic illustration of the growth models for a) nanorods, b) nanoplates, c) microrods, and d) dumbell-shaped (DB) microrods of zinc oxide.

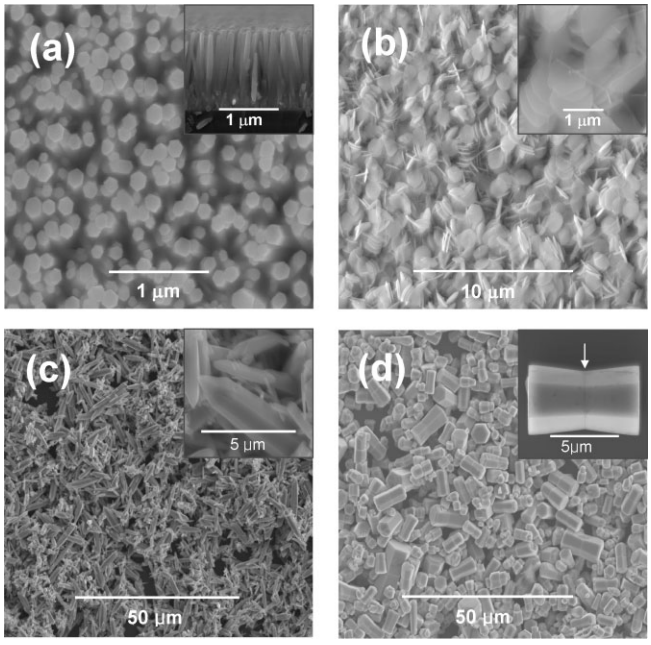

Figure 2. FESEM images of a) nanorods, b) nanoplates, c) microrods, and d) DB microrods of zinc oxide.

was much reduced, compared with that of the nanorod. In addition, the morphology of the microcrystals could be further tailored by the use of acetate-intercalated zinc hydroxy double salt (Zn-HDS) as an intermediate (Fig. 1d). By carrying out FESEM, high-resolution transmission electron microscopy/selected-area electron diffraction (HRTEM/SAED), and X-ray diffraction (XRD) analyses on the reaction intermediates,[9] it was determined that a fraction of the outermost surface of the Zn-HDS intermediate was transformed into hexagonal ZnO crystallites under hydrothermal conditions at 95 °C (the fraction depended on the pH variation of the nutrient solution), after which the surface-formed ZnO crystallites acted as nucleation centers for dumbbell-shaped ZnO microrods (hereafter referred to as DB microrods). Since the intercalated acetate anions in the Zn-HDS lattice were stabilized between the Zn (0001) planes through the formation of DB microrods, the Zn (0001) faces were completely masked. In fact, the FESEM image of Figure 2d reveals that the DB microrods were formed by co-sharing the acetate ligands, giving rise to the hybridization of two individual microrod crystals. One thing to note here is that both hexagonal microrods and DB microrods turn out to have a broader size distribution than the nanorods and nanoplates.

With the morphology-controlled ZnO, we were able to systematically investigate the relationship between crystal growth plane and photocatalytic activity. For this purpose, we monitored the concentration of H_2O_2 formed by a suspension of ZnO crystals under UV irradiation. As shown in the left panel of Figure 3, the ZnO nanoplates, with a higher ratio of polar to nonpolar faces, induced rapid generation of H_2O_2, up to 17 mM g^{-1}, under UV irradiation lasting for 730 min. Both the ZnO nanorods and microrods led to the formation of H_2O_2 upon UV irradiation but the formation rate was quite slow compared to that of the nanoplates. Out of both rod-shaped materials, the nanorods, which had a greater surface area of polar faces, showed slightly better activity than the microrods, which is consistent with their respective areas of polar faces (Table 1). This finding is an indication that an increase of polar Zn (0001) or O (000$\bar{1}$) faces leads to a significant enhancement of photocatalytic activity, whereas the area of nonpolar {01$\bar{1}$0} planes has negligible influence on the formation of H_2O_2. However, since the nanoplates possessed both the Zn (0001) and O (000$\bar{1}$) planes with the same concentration, it was difficult to differentiate which plane was responsible for the photocatalytic activity.

To achieve this differentiation, we also measured the photocatalytic activity of DB microrods with masked Zn (0001) faces. As can be seen clearly in the left panel of Figure 3, the H_2O_2 generation caused by the DB microrods was the lowest of all the samples. Although a DB microrod has the smallest surface area among the samples, its photocatalytic activity was even smaller than that of the hexagonal microrod with a similar surface area (Table 1). It is therefore concluded that the polar Zn (0001) plane was the most active site for photocatalytic H_2O_2 generation, even though the photocatalytic activity of the ZnO materials was not strictly quantitatively proportional to the surface area of the Zn (0001) face. This was possibly due to a crude estimation of surface area and/or a broad size distribution of the microcrystalline materials. To

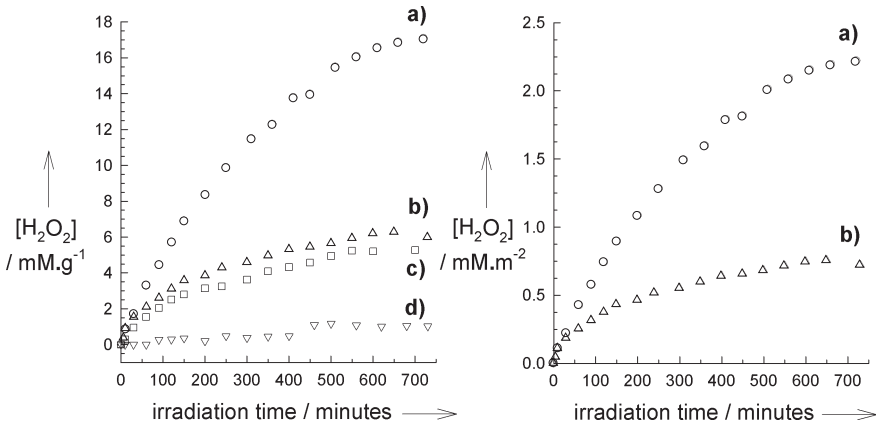

Figure 3. Time profiles of the evolution of H_2O_2 in UV-illuminated (wavelength $\lambda > 300$ nm) suspensions of a) nanoplates, b) nanorods, c) microrods, and d) DB microrods of zinc oxide. The left and right panels represent the weight- and surface-area-normalized data, respectively.

confirm this conclusion by ruling out the influence of total surface area on the photocatalytic efficiency, we compared the amount of H_2O_2 evolved after the normalization against the total surface area. As shown in the right panel of Figure 3, the nanoplates showed better activity than the nanorods, confirming the higher activity of the former morphology.[10] On the other hand, we found that under weak acidic conditions (pH 6.2 at 95 °C), the DB ZnO microrods were changed into plate-shaped crystals due to the sequential dissolution of the polar O $(000\bar{1})$ faces and the nonpolar $\{01\bar{1}0\}$ ones.[9] This result indicated strongly that the Zn (0001) face was more resistant to acidic corrosion than the other faces. Such a difference in the chemical stabilities of the faces would be partially responsible for the higher photocatalytic activity of the ZnO nanoplates, which have a high population of polar Zn (0001) faces.

In terms of the previously proposed mechanism for the photoinduced generation of H_2O_2, one can understand why the Zn (0001) plane is photocatalytically active. As M. R. Hoffmann and coworkers proposed, the mechanism for the photocatalytic generation of H_2O_2 can be explained as follows

$$ZnO + h\nu \rightarrow e_{cb}^- + h_{vb}^+ \quad (1)$$

$$O_2 + e_{cb}^- \rightarrow O_2^{\bullet -} \quad (2)$$

$$O_2^{\bullet -} + 2H^+ \rightarrow H_2O_2 + O_2 \quad (3)$$

$$CH_3COO^- + h_{vb}^+ \rightarrow CH_3^{\bullet} + CO_2 \quad (4)$$

where $h\nu$ is the energy of a photon, and h_{vb}^+ is a hole. A transient electron (e_{cb}^-) in the conduction band, generated by an excitation from the valence band, induces the formation of hydrogen peroxide through an intermediate peroxide radical.[3a] The reported Langmuirian dependence of quantum yield on oxygen pressure, and the results of ^{18}O isotropic labelling experiments, indicated that the partial formation of H_2O_2 occurs via the reduction of oxygen adsorbed on ZnO by conduction band electrons, as described in step 2.[3a] Considering the strong preference of Zn ions for a tetrahedral coordination geometry and the coordinatively unsaturated environment of Zn ions on the Zn (0001) plane, the higher photocatalytic activity of this plane for the H_2O_2 generation can be understood as a result of the facile adsorption of oxygen molecules on this face. It is worthwhile to note here that in the present experiment the ZnO crystals were immersed in an aqueous solution, in which the Zn ions on the Zn (0001) planes were preferentially coordinated by hydroxide anions. Therefore, to promote the reaction step 2, oxygen molecules should replace hydroxyl groups coordinatively adsorbed on the Zn (0001) planes. Previously it was reported that an adsorption of oxygen molecules onto the surface of ZnO is thermodynamically favorable, while an adsorption of hydroxyl groups is kinetically preferred.[11] In our experimental conditions, with O_2 bubbling, a high oxygen partial pressure effectively promoted the replacement of adsorbed hydroxide ions by oxygen molecules, and this is responsible for the effective generation of H_2O_2 observed. The hole (h_{vb}^+) formed in reaction step 1 reacted with a hole scavenger added (i.e., acetate), leading to the formation of a methyl radical and carbon dioxide, as described in step 4.[3b] Subsequently, the methyl radicals generated reacted with various species, such as O_2 and $HO_2^{\bullet}$, to produce several organic peroxides.[3b]

In summary, we were successful in synthesizing nanorods, nanoplates, microrods, and DB microrods of zinc oxide with different ratios of polar to nonpolar faces, through soft-solution processes. Also, we have clearly demonstrated that ZnO nanoplates with a high population of polar Zn (0001) faces show the highest photocatalytic activity for H_2O_2 generation, and that fine-tuning of face orientation results in optimization of the photocatalytic activity of nanostructured semiconductors.

Experimental

As the precursor for the nanoplates and nanorods, ZnO nanoparticles were prepared by a method previously developed by Spanhel and Anderson [12]. The nanoplates were synthesized from the nanoparticles by a soft-solution process at 95 °C for 24 h under a nutrient solution (100 mL) of 0.5 M $Zn(CH_3COO)_2{\cdot}2H_2O$, 0.1 M NaOH, and 0.17 mM sodium citrate. The nanorod array was prepared by hydrothermal treatment of dip-coated ZnO nanoparticles on a Si wafer [6a], and each nanorod was separated from the substrate by scratching, and then dispersed into the deionized water by ultrasoni-

ADVANCED MATERIALS

cating. The microrods were hydrothermally synthesized from aqueous solution (100 mL) of 1.0 M $Zn(CH_3COO)_2{\cdot}2\,H_2O$ and 2.0 M NaOH at 200 °C for 12 h. The DB microrods were synthesized from the aqueous solution of 0.1 M $Zn(CH_3COO)_2{\cdot}2\,H_2O$ and 0.1 M hexamethylenetetramine (HMTA) under hydrothermal conditions of 95 °C for 6 h. The crystal structure and crystallite morphology of the reaction intermediates in the synthesis of the DB crystals were studied by XRD, FESEM (JEOL JSM-6700F microscope), and HRTEM/SAED. To study the photocatalytic generation of H_2O_2, a 0.01 g ZnO sample was put into a 200 mL quartz cell containing of 120 mL of 2 mM acetate solution as a hole scavenger, and then the resulting suspension was continuously stirred under UV irradiation (300 W Xe lamp) and oxygen bubbling (30 mL min^{-1}). The time evolution of H_2O_2 concentration was examined by an iodide method [3], whose detection limit was approximately 10^{-6} mol. The concentration of triiodide ions (I_3^-) generated from four different stock solutions was determined from UV-vis absorption spectroscopy and the resulting standard calibration curve was used to estimate the H_2O_2 concentration.

Received: June 30, 2006
Revised: August 25, 2006

[1] R. Rife, T. W. Thomas, D. W. Norberg, R. L. Fournier, F. G. Rinker, M. S. Bonomo, *Environ. Prog.* **1989**, *8*, 167.
[2] M. R. Hoffmann, S. T. Martin, W. Choi, D. W. Bahnemann, *Chem. Rev.* **1995**, *95*, 69.
[3] a) A. J. Hoffmann, E. R. Carraway, M. R. Hoffmann, *Environ. Sci. Technol.* **1994**, *28*, 776. b) E. R. Carraway, A. J. Hoffmann, M. R. Hoffmann, *Environ. Sci. Technol.* **1994**, *28*, 786.
[4] K. Sato, M. Aoki, R. Noyori, *Science* **1998**, *281*, 1646.
[5] W.-J. Li, E.-W. Shi, W.-Z. Zhong, Z.-W. Yin, *J. Cryst. Growth* **1999**, *203*, 186.
[6] a) J.-H. Choy, E. -S. Jang, J.-H. Won, J.-H. Chung, D.-J. Jang, Y.-W. Kim, *Adv. Mater.* **2003**, *15*, 1911. b) J.-H. Choy, E.-S. Jang, J.-H. Won, J.-H. Chung, D.-J. Jang, Y.-W. Kim, *Appl. Phys. Lett.* **2004**, *84*, 287.
[7] Z. R. Tian, J. A. Voigt, B. McKenzie, M. J. McDermott, *J. Am. Chem. Soc.* **2002**, *124*, 12 954.
[8] Z. R. Tian, J. A. Voigt, J. Liu, B. McKenzie, M. J. McDermott, M. A. Rodriguez, H. Konishi, H. Xu, *Nat. Mater.* **2003**, *2*, 821.
[9] Please see Supporting Information.
[10] After the normalization of activity data against the total surface area, the microcrystalline rods and DB rods of ZnO seem to produce a larger amount of H_2O_2 than the nanostructured ZnO compounds. However, due to the very small surface area of the microcrystalline ZnO, a quantity more than 16 times larger is required in order to have the equivalent total surface area to that of nanocrystalline ZnO. In light of this, the observed higher activity of the microcrystalline zinc oxides in the surface-area-normalized plot (not shown in the text) should be interpreted as a result of their larger quantity rather than of their intrinsic high activity. Although normalization by the total surface area makes the amount of zinc oxide on the surface identical for all the materials under investigation, the quantity of zinc oxide in the bulk becomes much larger for the microcrystalline samples than for the nanocrystalline homologues. It is well known that holes and excited electrons can be formed not only on the surface but also in the bulk, and both can take part in photocatalysis.
[11] R.-D. Sun, A. Nakajima, A. Fujishima, T. Watanabe, K. Hashimoto, *J. Phys. Chem. B* **2001**, *105*, 1984.
[12] L. Spanhel, M. A. Anderson, *J. Am. Chem. Soc.* **1991**, *113*, 2826.

